Inorg. Chem. **2006**, *45*, 6041–6047

Transformation and Structural Discrimination between the Neutral $\{Fe(NO)_2\}^{10}$ Dinitrosyliron Complexes (DNICs) and the Anionic/Cationic $\{Fe(NO)_2\}^9$ DNICs

Mu-Cheng Hung,[†] Ming-Che Tsai,[†] Gene-Hsiang Lee,[‡] and Wen-Feng Liaw*[,†]

Department of Chemistry, National Tsing Hua University, Hsinchu 30013, Taiwan, and Instrumentation Center, National Taiwan University, Taipei, Taiwan

Received March 27, 2006

Reaction of $Fe(CO)_2(NO)_2$ and sparteine/tetramethylethylenediamine (TMEDA) in tetrahydrofuran afforded the electron paramagnetic resonance (EPR)-silent, neutral $\{Fe(NO)_2\}^{10}$ dinitrosyliron complexes (DNICs) [(sparteine)$Fe(NO)_2$] (**1**) and [(TMEDA)$Fe(NO)_2$] (**2**), respectively. The stable and isolable anionic $\{Fe(NO)_2\}^9$ DNIC $[(S(CH_2)_3S)Fe(NO)_2]^-$ (**4**), with a bidentate alkylthiolate coordinated to a $\{Fe(NO)_2\}$ motif, was prepared by the reaction of $[S(CH_2)_3S]^{2-}$ and the cationic $\{Fe(NO)_2\}^9$ $[(sparteine)Fe(NO)_2]^+$ (**3**) obtained from the reaction of complex **1** and $[NO][BF_4]$ in CH_3CN. Transformation from the neutral complex **1** to the anionic complex **4** was verified via the cationic complex **3**. Here complex **3** acts as an $\{Fe(NO)_2\}$-donor reagent in the presence of thiolates. The EPR spectra of complexes **3** and **4** exhibit an isotropic signal with $g = 2.032$ and 2.031 at 298 K, respectively, the characteristic g value of $\{Fe(NO)_2\}^9$ DNICs. On the basis of N–O/Fe–N(O) bond lengths of the single-crystal X-ray structures of the $\{Fe(NO)_2\}^9/\{Fe(NO)_2\}^{10}$ DNICs, the oxidation level of the $\{Fe(NO)_2\}$ core of DNICs can be unambiguously assigned. The mean N–O distances falling in the range of 1.214(6)–1.189(4) Å and the Fe–N(O) bond distances in the range of 1.650(7)–1.638(3) Å are assigned as the neutral $\{Fe(NO)_2\}^{10}$ DNICs. In contrast, the mean N–O bond distances ranging from 1.178(3) to 1.160(6) Å and the mean Fe–N(O) bond distances ranging from 1.695(3) to 1.661(4) Å are assigned as the anionic/neutral/cationic $\{Fe(NO)_2\}^9$ DNICs. In addition, an EPR spectrum in combination with the IR ν_{NO} (the relative position of the ν_{NO} stretching frequencies and their difference $\Delta\nu_{NO}$) spectrum may serve as an efficient tool for discrimination of the existence of the anionic/cationic/neutral $\{Fe(NO)_2\}^9$ DNICs and the neutral $\{Fe(NO)_2\}^{10}$ DNICs.

Introduction

Dinitrosyliron complexes (DNICs) have been suggested as intermediates of Fe-catalyzed degradation and formation of *S*-nitrosothiols (RSNO) and as one of two possible forms for storage and transport of NO in biological systems.[1] Depending on the microenvironment, low-molecular-weight DNICs (LMW-DNICs) can provide at least two types of nitrosylating modifications of proteins, forming either protein/*S*-nitrosothiols or protein-bound DNICs.[1,2] As observed in cells or tissues, LMW-DNICs exerting cyclic GMP (guanosine monophosphate)-independent effects were attributed to nitrosylating modification of proteins via the transfer of NO or a $Fe(NO)_2$ unit, yielding protein/*S*-nitrosothiols or protein-bound DNICs.[3,4] In particular, the protein-bound DNICs were characterized by X-ray crystallography through nitrosylation of human glutathione transferase P1-1 with a dinitrosyldiglutathionyliron complex in vitro/in vivo recently.[4]

As has been known, characterization of both protein-bound and LMW-DNICs in vitro has been made possible via their

* To whom correspondence should be addressed. E-mail: wfliaw@mx.nthu.edu.tw.

[†] National Tsing Hua University.

[‡] National Taiwan University.

(1) (a) Stamler, J. S. *Cell* **1994**, *78*, 931−936. (b) Stamler, J. S.; Singel, D. J.; Loscalzo, J. *Science* **1992**, *258*, 1898−1902. (c) Ford, P. C.; Lorkovic, I. M. *Chem. Rev.* **2002**, *102*, 993−1017. (d) Butler, A. R.; Megson, I. L. *Chem. Rev.* **2002** *102*, 1155−1166. (e) Ueno, T.; Susuki, Y.; Fujii, S.; Vanin, A. F.; Yoshimura, T. *Biochem. Pharmacol.* **2002**, *63*, 485−493. (f) Lee, J.; Chen, L.; West, A. H.; Richter-Addo, G. B. *Chem. Rev.* **2002**, *102*, 1019−1065. (g) McCleverty, J. A. *Chem. Rev.* **2004**, *104*, 403−418. (h) Hayton, T. W.; Legzdins, P.; Sharp, W. B. *Chem. Rev.* **2002**, *102*, 935−991. (i) Wang, P. G.; Xian, M.; Tang, X.; Wu, X.; Wen, Z.; Cai, T.; Janczuk, A. J. *Chem. Rev.* **2002**, *102*, 1091−1134.

(2) (a) Badorff, C.; Fichtlscherer, B.; Muelsch, A.; Zeiher, A. M.; Dimmeler, S. *Nitric Oxide* **2002**, *6*, 305−312. (b) Mulsch, A.; Mordvintcev, P. I.; Vanin, A. F.; Busse, R. *FEBS Lett.* **1991**, *294*, 252−256.

(3) (a) Wiegant, F. A. C.; Malyshev, I. Y.; Kleschyov, A. L.; van Faassen, E.; Vanin, A. F. *FEBS Lett.* **1999**, *455*, 179−182. (b) Schmidt, H. H. H. W. *FEBS Lett.* **1992**, *307*, 102−107.

(4) Cesareo, E.; Parker, L. J.; Pedersen, J. Z.; Nuccetelli, M.; Mazzetti, A. P.; Pastore, A.; Federici, G.; Caccuri, A. M.; Ricci, G.; Adams, J. J.; Parker, M. W.; Bello, M. L. *J. Biol. Chem.* **2005**, *280*, 42172−42180.

10.1021/ic0605120 CCC: $33.50
Published on Web 06/22/2006

distinctive electron paramagnetic resonance (EPR) signals at $g = 2.03$.[1−5] To our knowledge, also known in inorganic chemistry is the precedents for small-molecule DNICs in four oxidation levels of the $\{Fe(NO)_2\}$ unit, including the EPR-active, anionic $\{Fe(NO)_2\}$,[9] neutral $\{Fe(NO)_2\}$,[9] and cationic $\{Fe(NO)_2\}^9$ DNICs as well as the EPR-silent, neutral $\{Fe(NO)_2\}^{10}$ DNICs coordinated by CO, PPh_3, and N-containing ligands.[6−10] Here the electronic structure/state of the $M(NO)_2$ unit of DNICs is generally designated as $\{M(NO)_2\}^n$ (M = transition metal).[7] This formalism $\{M(NO)_2\}^n$ invokes the Enemark−Feltham notation, which stresses the well-known covalency and delocalization in the electronically amorphous $M(NO)_2$ unit.[7]

Recently, we have shown that the detailed spectroscopic analysis (EPR and IR ν_{NO} spectra) may provide a superior level of insight on discrimination of the anionic $\{Fe(NO)_2\}^9$ DNICs, neutral $\{Fe(NO)_2\}^9$ DNIC [(SC_6H_4-*o*-NHCOPh)(1-MeIm)$Fe(NO)_2$] (1-MeIm = 1-methylimidazole), and Roussin's red ester[10a] and that the reversible transformation of complex $[S_5Fe(NO)_2]^-$ to the $[S_5Fe(\mu\text{-}S)_2FeS_5]^{2-}$ cluster by photolysis in the presence of the NO-acceptor reagent $[(C_4H_8O)Fe(S,S\text{-}C_6H_4)_2]^-$ is consistent with reports of in vitro repair of nitric oxide modified [2Fe−2S] ferredoxin by cysteine desulfurase and L-cysteine.[10b,11] We also demonstrated that the NO-releasing ability of the anionic $\{Fe(NO)_2\}^9$ $[(RS)_2Fe(NO)_2]^-$ is finely tuned by the coordinated thiolate ligands.[10c] Because of the lack of isolation and X-ray structural data for the anionic $\{Fe(NO)_2\}^9$ DNICs $[(RS)_2Fe(NO)_2]^-$ containing alkylthiolate ligands coordinated to the Fe reported,[12] the property and reactivity of alkylthiolate-containing DNICs have not been explored. Also, elucidation of the structural features of the $\{Fe(NO)_2\}^{10}/\{Fe(NO)_2\}^9$ DNICs is important for the chemical understanding of these species. The objective of this study was to delineate the syntheses/reactivity of the neutral $\{Fe(NO)_2\}^{10}$ DNICs [(L)$Fe(NO)_2$] [L = sparteine (**1**), tetramethylethylenediamine (TMEDA; **2**)] and the anionic $\{Fe(NO)_2\}^9$ DNIC $[(S(CH_2)_3S)Fe(NO)_2]^-$ (**4**) containing a bidentate alkylthiolate ligand coordinated to the $\{Fe(NO)_2\}$ unit and to investigate the transformation of complex **1** into complex **4** via a cationic $\{Fe(NO)_2\}^9$ DNIC [(sparteine)$Fe(NO)_2$]$^+$ (**3**). Of importance, the structural discrimination between the $\{Fe(NO)_2\}^{10}$ and $\{Fe(NO)_2\}^9$ DNICs was concluded.

Results and Discussion

Syntheses of the Neutral $\{Fe(NO)_2\}^{10}$ [(Sparteine)Fe(NO)$_2$] (1) and [(TMEDA)Fe(NO)$_2$] (2). Reaction of $Fe(CO)_2(NO)_2$ (0.2 mmol)[13] and sparteine (0.2 mmol) in tetrahydrofuran (THF) at ambient temperature yielded the EPR-silent, neutral $\{Fe(NO)_2\}^{10}$ DNIC **1** isolated as a green solid (35% yield) and characterized by IR, UV−vis, EPR, and single-crystal X-ray diffraction. Complex **1** exhibits diagnostic IR ν_{NO} stretching frequencies at 1622 (vs) and 1679 (vs) cm^{-1} (CH_3CN) and 1633 (vs) and 1687 (vs) cm^{-1} (THF).[8,9] In a similar fashion, synthesis of the green, neutral $\{Fe(NO)_2\}^{10}$ DNIC **2** by reaction of $Fe(CO)_2(NO)_2$ and TMEDA in 1:1 stoichiometry was investigated in THF under a N_2 atmosphere at ambient temperature. The shifts of IR ν_{NO} to higher wavenumbers in complex **2** [ν_{NO} 1644 (vs) and 1698 (vs) cm^{-1} (THF)] as compared to complex **1** show the less electron-donating character of TMEDA as compared to that of sparteine. The stretching frequencies ν_{NO} of complexes **1** and **2** fall into the range from 1758 and 1807 cm^{-1} (THF) for the thermally unstable $[(CO)_2Fe(NO)_2]$ to 1616 and 1673 cm^{-1} for the isolable $[(1\text{-MeIm})_2Fe(NO)_2]$.[9,13] In contrast to the anionic $\{Fe(NO)_2\}^9$ DNICs $[(RS)_2Fe(NO)_2]^-$,[10c] the $\{Fe(NO)_2\}$ motif of the neutral $\{Fe(NO)_2\}^{10}$ DNICs shows more affinity for the stronger electron-donating ligands to yield the stable/isolable neutral $[(L)_2Fe(NO)_2]$ (L = N-containing ligands). Complexes **1** and **2** are soluble in THF/CH_3CN and exhibit air sensitivity in solution but are stable to air for hours in the solid state.

Conversion of the Neutral 1 into the Anionic $\{Fe(NO)_2\}^9$ 4 and [Fe$_2$(μ-SPh)$_2$(NO)$_4$] (5). As presented in Scheme 1a, upon the addition of $[NO][BF_4]$ into a CH_3CN solution of complex **1** in a 1:1 stoichiometry, a reaction ensued over the course of 5 min to yield the cationic $\{Fe(NO)_2\}^9$ **3** identified by EPR and IR spectra. The EPR spectrum of complex **3** exhibits an isotropic signal with $g = 2.032$ at 298 K (Figure 1), the characteristic g value of $\{Fe(NO)_2\}^9$ DNICs. The shift in ν_{NO} from 1622 (vs) and 1679 (vs) cm^{-1} (CH_3CN) (**1**) to 1746 (vs) and 1814 (vs) cm^{-1} (CH_3CN) is in accordance with the formation of complex **3**.[14] Complex **3** is unstable and decomposes spontaneously to an insoluble solid over the period of 5 h. We noticed that the lifetimes of the cationic $\{Fe(NO)_2\}^9$ DNICs depend strongly on the structure (monodentate/bidentate) and electron-donating ability of the coordinated ligands (sparteine vs TMEDA; sparteine vs PPh_3) because the cationic $\{Fe(NO)_2\}^9$ [(TMEDA)$Fe(NO)_2$]$^+$ cannot be observed spectrally (by EPR or IR) at room temperature, whereas the cationic $\{Fe(NO)_2\}^9$ $[(Ph_3P)_2Fe(NO)_2]^+$ was isolated and characterized by single-crystal X-ray diffraction.[14]

(5) (a) Foster, M. W.; Cowan, J. A. *J. Am. Chem. Soc*. **1999**, *121*, 4093−4100. (b) Lancaster, J. R., Jr.; Hibbs, J. B., Jr. *Proc. Natl. Acad. Sci. U.S.A.* **1990**, *87*, 1223−1227.

(6) (a) Chiang, C.-Y.; Miller, M. L.; Reibenspies, J. H.; Darensbourg, M. Y. *J. Am. Chem. Soc.* **2004**, *126*, 10867−10874. (b) Baltusis, L. M.; Karlin, K. D.; Rabinowitz, H. N.; Dewan, J. C.; Lippard, S. J. *Inorg. Chem*. **1980**, *19*, 2627−2632.

(7) Enemark, J. H.; Feltham, R. D. *Coord. Chem. Rev.* **1974**, *13*, 339−406.

(8) Albano, V. G.; Araneo, A.; Bellon, P. L.; Ciani, G.; Manassero, M. *J. Organomet. Chem*. **1974**, *67*, 413−422.

(9) Reginato, N.; McCrory, C. T. C.; Pervitsky, D.; Li, L. *J. Am. Chem. Soc*. **1999**, *121*, 10217−10218.

(10) (a) Tsai, M.-L.; Liaw, W.-F., submitted for publication. (b) Tsai, M.-L.; Chen, C.-C.; Hsu, I.-J.; Ke, S.-C.; Hsieh, C.-H.; Chiang, K.-A.; Lee, G.-H.; Wang, Y.; Liaw, W.-F. *Inorg. Chem.* **2004**, *43*, 5159−5167. (c) Tsai, F.-T.; Chiou, S.-J.; Tsai, M.-C.; Tsai, M.-L.; Huang, H.-W.; Chiang, M.-H.; Liaw, W.-F. *Inorg. Chem*. **2005**, *44*, 5872−5881. (d) Chen, T.-N.; Lo, F.-C.; Tsai, M.-L.; Shih, K.-N.; Chiang, M.-H.; Lee, G.-H.; Liaw, W.-F. *Inorg. Chim. Acta* **2006**, *359*, 2525−2533.

(11) (a) Yang, W.; Rogers, P. A.; Ding, H. *J. Biol. Chem*. **2002**, *277*, 12868−12873. (b) Rogers, P. A.; Ding, H. *J. Biol. Chem*. **2001**, *276*, 30980−30986.

(12) Jaworska, M.; Stasicka, Z. *J. Organomet. Chem.* **2004**, *689*, 1702−1713.

(13) McBride, D. W.; Stafford, S. L.; Stone, F. G. A. *Inorg. Chem*. **1962**, *1*, 386−388.

(14) Atkinson, F. L.; Blackwell, H. E.; Brown, N. C.; Connelly, N. G.; Crossley, J. G.; Orpen, A. G.; Rieger, A. L.; Rieger, P. H. *J. Chem. Soc., Dalton Trans.* **1996**, 3491−3502.

Scheme 1

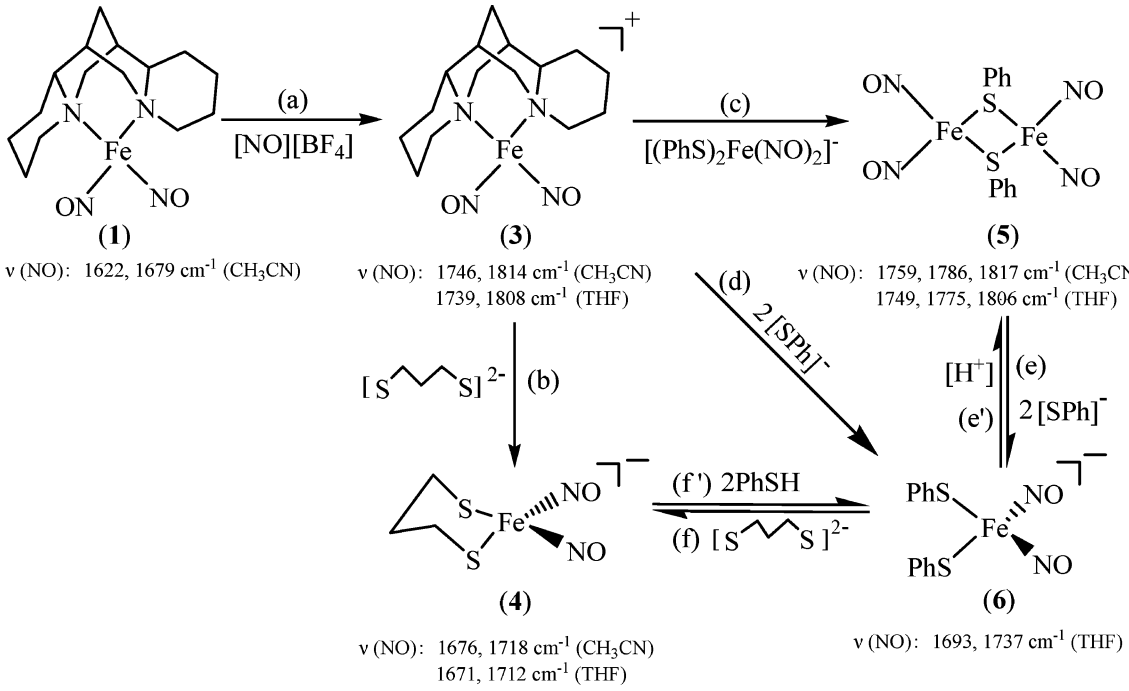

Upon the addition of 1 equiv of $[S(CH_2)_3S]^{2-}$ to the CH_3CN solution of complex **3**, a pronounced color change from green to dark brown occurs under N_2 at ambient temperature. The IR, UV−vis, EPR, SQUID, and single-crystal X-ray diffraction studies confirmed the formation of the anionic $\{Fe(NO)_2\}^9$ DNIC **4** (yield 63%) with a bidentate alkylthiolate ligand $[S(CH_2)_3S]^{2-}$ coordinated to the $\{Fe(NO)_2\}^9$ motif (Scheme 1b). This result demonstrates that the facile conversion of complex **1** to the anionic complex **4** was carried out via the intermediate, the cationic complex **3**. The cationic complex **3** acting as an $\{Fe(NO)_2\}^9$-donor reagent was also displayed by the reaction of complex **3** and $[(PhS)_2Fe(NO)_2]^-$ (**6**); the shift in ν_{NO} from 1746 and 1814 cm^{-1} (**3**) to 1759 (s), 1786 (s), and 1817 (w) cm^{-1} (CH_3CN) is in accordance with the formation of the EPR-silent, Roussin's red ester **5** (Scheme 1c).[15]

The surprisingly stable complex **4** is the first example of the anionic $\{Fe(NO)_2\}^9$ DNICs containing alkylthiolate coordinated to the $\{Fe(NO)_2\}^9$ motif isolated and characterized by single-crystal X-ray diffraction.[6,12] This complex represents an important starting point to understand the factors that are responsible for the stability and reactivity of the anionic $\{Fe(NO)_2\}^9$ alkylthiolate-containing DNICs. The IR spectrum of complex **4** in THF reveals two ν_{NO} stretching bands at 1671 (s) and 1712 (s) cm^{-1}. We noticed that the IR spectra for the cationic complex **3** and the anionic complex **4** had the same pattern but differed in position [1746 and 1814 cm^{-1} for **3** versus 1676 and 1718 cm^{-1} for **4** (CH_3CN)] and separation of NO stretching frequencies ($\Delta\nu_{NO}$ = 68 cm^{-1} for **3** versus 42 cm^{-1} for **4**). At 298 K, complex **4** exhibits an isotropic EPR signal at $g = 2.031$ (Figure 2). As observed in the previous study,[10c] the temperature-dependent effective magnetic moment [the effective magnetic moment (μ_{eff}) decreases from 2.25 μ_B at 300 K to 1.17 μ_B at 4 K] of complex **4** may be contributed from both $\{Fe^+(^{\bullet}NO)_2\}^9$ ($S_T = {}^5/_2$) and $\{Fe^-(^+NO)_2\}^9$ ($S_T = {}^1/_2$) electronic states. Complex **4** was alternatively obtained via a bridged-ligand breakage reaction, a straightforward reaction of complex $[Fe_2(\mu\text{-}S(CH_2)_3S)(NO)_4]$ with 1 equiv of $[S(CH_2)_3S]^{2-}$ in THF. The quantitative conversion of complex $[Fe_2(\mu\text{-}S(CH_2)_3S)(NO)_4]$ to **4** was monitored by Fourier transform infrared (FTIR); the ν_{NO} stretching bands 1749 (s), 1775 (s), and 1806 (vw) cm^{-1} (complex $[Fe_2(\mu\text{-}S(CH_2)_3S)(NO)_4]$) disappeared accompanied by the simultaneous formation of the stretching bands 1671 (s) and 1712 (s) cm^{-1}.

Interestingly, the formation of complex $[Fe_2(\mu\text{-}SEt)_2(NO)_4]$ [1750 (s), 1776 (s), 1807 (vw) cm^{-1} (CH_3CN)] was observed when complex **3** was treated with 2 equiv of $[SEt]^-$ in CH_3CN at ambient temperature.[6,15] This result shows that the reaction of complex **3** with nucleophile $[SEt]^-$ occurs initially

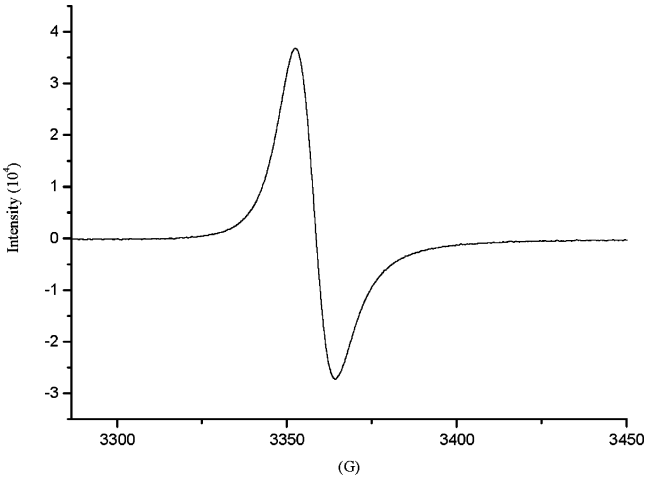

Figure 1. EPR spectrum of complex **3** with $g = 2.032$ at 298 K.

(15) Rauchfuss, T. B.; Weatherill, T. D. *Inorg. Chem.* **1982**, *21*, 827−830.

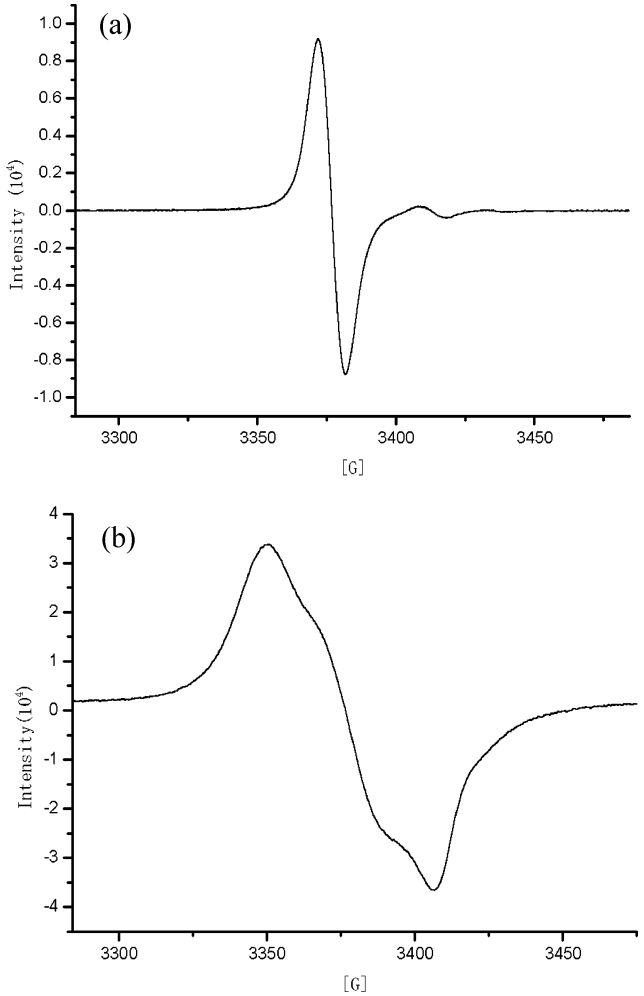

Figure 2. EPR spectrum of complex **4** (a) with an isotropic $g_{av} = 2.031$ signal at 298 K and (b) with a rhombic $g_x = 2.048$, $g_y = 2.033$, $g_z = 2.015$ signal at 77 K.

at the more accessible electrophile $[Fe(NO)_2]^+$ to yield the charge-controlled, collision product $[(EtS)_2Fe(NO)_2]^-$, which subsequently transformed into the more stable form, complex $[Fe_2(\mu\text{-}SEt)_2(NO)_4]$. Obviously, the two alkylthiolates $[S(CH_2)_3S]^{2-}$ and $[SEt]^-$, rendering the $\{Fe(NO)_2\}^9$ unit in different structural environments, induce differing stability to $\{Fe(NO)_2\}^9$ fragment. In contrast, the coordinated sparteine ligand of complex **3** could also be replaced by thiolate $[SPh]^-$. As shown in Scheme 1d, reaction of complex **3** and 2 equiv of $[SPh]^-$ in a CH_3CN solution at room temperature rapidly yielded the known **6** characterized by IR, UV−vis, and EPR.[10c,16] These results in combination with the previous study elucidate that not only electronic but also structural environments of the coordinated thiolate ligands of the anionic $\{Fe(NO)_2\}^9$ DNICs play a key role in creating/stabilizing DNICs. The ν_{NO} stretching frequencies [1671 and 1712 cm^{-1} (THF)] observed in complex **4** fall out of the range from 1716 and 1766 cm^{-1} to 1693 and 1737 cm^{-1} observed in the known stable and isolable $\{Fe(NO)_2\}^9$ $[(RS)_2Fe(NO)_2]^-$.[10c] The chelating effect of $[S(CH_2)_3S]^{2-}$ coordinated to the $\{Fe(NO)_2\}$ motif overwhelming the

(16) Strasdeit, H.; Krebs, B.; Henkel, G. *Z. Naturforsch.* **1986**, *41b*, 1357−1362.

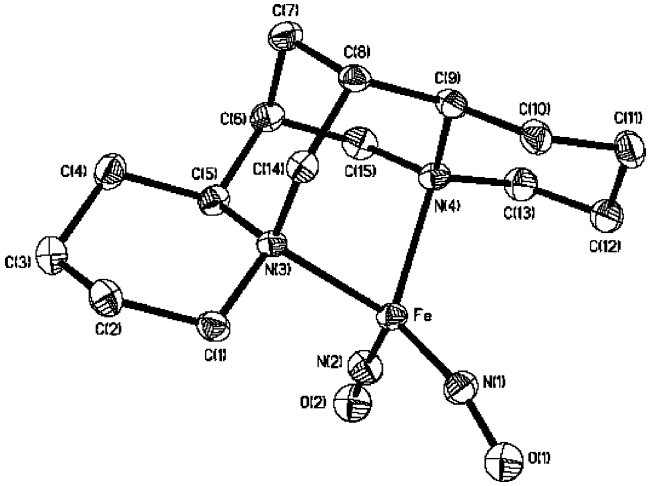

Figure 3. ORTEP drawing and labeling scheme of **1** with thermal ellipsoids drawn at 50% probability. Selected bond distances (Å) and angles (deg): Fe−N(1), 1.6501(19); Fe−N(2), 1.6430(19); Fe−N(3), 2.1324(17); Fe−N(4), 2.1319(18); N(1)−O(1), 1.206(6); N(1)−O(1′), 1.220(6); N(2)−O(2), 1.214(5); N(2)−O(2′), 1.217(5); N(2)−Fe−N(1), 112.08(10); N(2)−Fe−N(4), 105.90(8); N(1)−Fe−N(4), 121.63(8); N(2)−Fe−N(3), 114.82(8); N(1)−Fe−N(3), 115.59(8); N(4)−Fe−N(3), 84.03(7); O(1)−N(1)−O(1′), 14.0(4); O(1)−N(1)−Fe, 160.1(3); O(1′)−N(1)−Fe, 167.1(3); O(2)−N(2)−O(2′), 18.9(3); O(2)−N(2)−Fe, 176.0(3); O(2′)−N(2)−Fe, 159.0(3).

electronic effect (electron-donating ability of thiolates) may rationalize the stability/isolation of complex **4**.

Reversibly, quantitative transformation of complex **5** to **6** was monitored by IR ν_{NO} spectroscopy; the shift of the stretching frequencies from 1749 (s), 1775 (s), and 1806 (w) cm^{-1} to the lower wavenumbers 1693 (s) and 1737 (s) cm^{-1} confirmed the formation of complex **6** (yield 86%) when a THF solution of the dinuclear **5** was reacted with 2 equiv of $[SPh]^-$ (Scheme 1e).[10a] Complex **4** does not react with $[SPh]^-$ via thiolate ligand exchange to form complex **6**.[10c] In contrast, the coordinated $[SPh]^-$ ligands of complex **6** could be replaced by the stronger electron-donating bidentate thiolate $[S(CH_2)_3S]^{2-}$ to yield complex **4** when reacting complex **6** with $[S(CH_2)_3S]^{2-}$ in THF at ambient temperature, as shown in Scheme 1f.[10c] The conversion of complex **4** to complex **6** was expected to be driven by protonation (PhSH) of complex **4**; the reaction of complex **4** and 2 equiv of thiophenol in THF does lead to isolation of the stable complex **6**. Presumably, protonation (electrophilic reaction of PhSH) of complex **4** by thiophenol occurs only at the more accessible, electron-rich sulfur site to form the well-known complex **6** (yield 82%) at ambient temperature (Scheme 1f′). Obviously, complex **4** containing the coordinated alkylthiolate ligand and complex **6** containing the coordinated phenylthiolate ligands are chemically interconvertible.

Structures. Figures 3 and 4 display thermal ellipsoid plots of the neutral complexes **1** and **2**, respectively, and selected bond distances and angles are given in the figure captions. The strain effect of the chelating ligand in the coordination sphere of complexes **1** and **2** explains that the geometry of Fe is a distorted tetrahedral with N(3)−Fe−N(4) bond angles of 84.03(7) and 82.57(12)°, respectively. The most striking feature of the neutral $\{Fe(NO)_2\}^{10}$ DNICs and anionic $\{Fe(NO)_2\}^9$ DNICs is the difference of Fe−N(O)/N−O bond lengths between the neutral $\{Fe(NO)_2\}^{10}$ and the anionic/

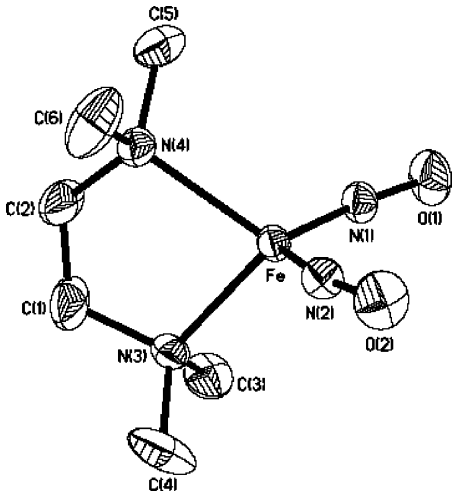

Figure 4. ORTEP drawing and labeling scheme of $[(CH_3)_2N(CH_2)_2N(CH_3)_2)Fe(NO)_2]$ with thermal ellipsoids drawn at 30% probability. Selected bond distances (Å) and angles (deg): Fe−N(1), 1.639(3); Fe−N(2), 1.637(3); Fe−N(3), 2.117(3); Fe−N(4), 2.109(3); N(1)−O(1), 1.188(4); N(2)−O(2), 1.197(4); N(2)−Fe−N(1), 115.36(16); N(2)−Fe−N(4), 115.26(15); N(1)−Fe−N(4), 112.54(15); N(2)−Fe−N(3), 114.81(14); N(1)−Fe−N(3), 112.10(15); N(4)−Fe−N(3), 82.57(12); O(1)−N(1)−Fe, 169.9(3); O(2)−N(2)−Fe, 166.9(3).

Table 1. Selected Fe−N(O) and N−O Bond Lengths for the Neutral {Fe(NO)$_2$}^{10} and the Anionic/Neutral/Cationic {Fe(NO)$_2$}^{9} DNICs

	Fe−N(O) (average) (Å)	N−O (average) (Å)	ref
Neutral {Fe(NO)$_2$}^{10} DNICs			
1	1.647(2)	1.214(6)	this work
2	1.638(3)	1.193(4)	this work
$[(1\text{-MeIm})_2Fe(NO)_2]$	1.649(3)	1.189(4)	9
$[(PPh_3)_2Fe(NO)_2]$	1.650(7)	1.190(10)	8a
Anionic/Neutral {Fe(NO)$_2$}^{9} DNICs			
4	1.676(2)	1.178(3)	this work
$[S_5Fe(NO)_2]^-$	1.678(3)	1.178(3)	10b
$[(2\text{-}S{-}(C_4H_3S)_2Fe(NO)_2]^-$	1.683(2)	1.178(2)	10c
$[(2\text{-}S{-}C_7H_4NS)_2Fe(NO)_2]^-$	1.684(6)	1.174(6)	10c
$[(SC_6H_4\text{-}o\text{-}NHCOCH_3)_2Fe(NO)_2]^-$	1.682(2)	1.170(3)	10c
$[(SePh)_2Fe(NO)_2]^-$	1.669(4)	1.162(5)	18
$[Se_5Fe(NO)_2]^-$	1.675(4)	1.170(5)	10d
$[(6\text{-}Me_3\text{-}TPA)Fe(NO)_2]^+$	1.695(3)	1.167(4)	17
$[(PPh_3)_2Fe(NO)_2]^+$	1.661(4)	1.160(6)	14
$[(PPh_3)(OPPh_3)Fe(NO)_2]^+$	1.668(13)	1.171(18)	14
$[(SC_6H_4\text{-}o\text{-}NHCOPh)(Im)Fe(NO)_2]$	1.683(6)	1.167(6)	10a
$[(H^+bme\text{-}daco)Fe(NO)_2]$	1.669(6)	1.186(7)	6a
$[(C_9H_{21}N_2S_2)Fe(NO)_2]$	1.680(3)	1.161(4)	6b

neutral {Fe(NO)$_2$}^{9} DNICs (Table 1). Compared to complex **4**, the mean N−O distances in complexes **1** and **2** have increased by 0.037 and 0.015 Å and the mean Fe−N(O) distances have decreased by 0.029 and 0.038 Å, respectively. Specifically, the mean N−O distances fall in the range of 1.214(6)−1.189(4) Å and the mean Fe−N(O) distances are within the range of 1.650(7)−1.638(3) Å for the neutral {Fe(NO)$_2$}^{10} DNICs, compared to the mean N−O distances ranging from 1.178(3) to 1.160(6) Å and the mean Fe−N(O) distances ranging from 1.695(3) to 1.661(4) Å for the anionic/neutral/cationic {Fe(NO)$_2$}^{9} DNICs (Table 1).

Figure 5 displays the thermal ellipsoid plot of the anionic complex **4**, and selected bond distances and angles are given in the figure caption. The X-ray structural determination of complex **4** shows that the $[FeS_2C_3]$ ring is in the chair conformation, similar to that found in complex $[(NO)_2Fe(S_5)]^-$.[10b] The constraint of the bidentate $[S(CH_2)_3S]^{2-}$ ligand generates a 100.92(2)° S(2)−Fe−S(1) angle, enforcing a significant distortion from a tetrahedral at the four-coordinated Fe site in complex **4**. The difference [ΔFe−N(O) = 0.007 Å] of the Fe−N(O) bond distance between complex **4** [average 1.676(2) Å for complex **4**] and the reported anionic $[(NO)_2Fe(SR)_2]^-$ containing the coordinated phenylthiolates $\{[(NO)_2Fe(2\text{-}S{-}C_7H_4NS)_2]^-$ [average 1.684(7) Å], $[(NO)_2Fe(SC_6H_4\text{-}o\text{-}NHC(O)CH_3)_2]^-$ [average 1.682(2) Å], and $[(NO)_2Fe(2\text{-}S{-}C_4H_3S)_2]^-$ [average 1.683(2) Å]$\}$[10c] may be attributed to the shorter Fe−S bond distance [average 2.2576(7) Å; the stronger electron-donating $[S(CH_2)_3S]^{2-}$ ligand] of complex **4** compared to those of 2.294(2), 2.301(1), and 2.2962(6) Å of complexes $[(NO)_2Fe(2\text{-}S{-}C_7H_4NS)_2]^-$, $[(NO)_2Fe(SC_6H_4\text{-}o\text{-}NHC(O)CH_3)_2]^-$, and $[(NO)_2Fe(2\text{-}S{-}C_4H_3S)_2]^-$, respectively.[10c] The mean value of the N−O bond lengths in complex **4** is 1.178(3) Å, slightly longer than those in complexes $[(NO)_2Fe(2\text{-}S{-}C_7H_4NS)_2]^-$ [average 1.174(6) Å] and $[(NO)_2Fe(SC_6H_4\text{-}o\text{-}NHC(O)CH_3)_2]^-$ [average 1.170(3) Å]. The Fe−N−O bond angle of 170.1(3)° (average) in complex **4** is comparable to the Fe−N−O bond angles of 169.7(5) (average) and 168.3(2)° (average) observed in $[(NO)_2Fe(2\text{-}S{-}C_7H_4NS)_2]^-$ and $[(NO)_2Fe(2\text{-}S{-}C_4H_3S)_2]^-$,[10c] respectively.

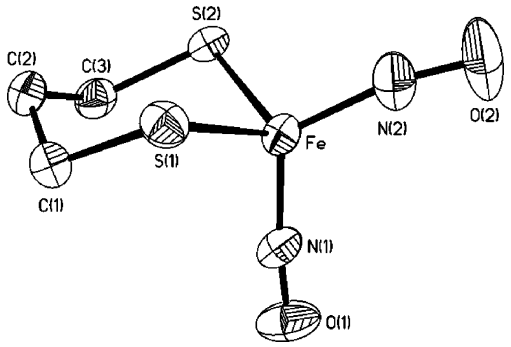

Figure 5. ORTEP drawing and labeling scheme of **4** with thermal ellipsoids drawn at 50% probability. Selected bond distances (Å) and angles (deg): Fe−N(1), 1.674(2); Fe−N(2), 1.677(2); Fe−S(1), 2.2609(7); Fe−S(2), 2.2544(7); N(1)−O(1), 1.181(3); N(2)−O(2), 1.174(3); N(2)−Fe−N(1), 118.61(11); N(1)−Fe−S(2), 107.59(7); N(2)−Fe−S(2) 107.90(8); N(1)−Fe−S(1), 108.54(7); N(2)−Fe−S(1), 111.72(8); S(2)−Fe−S(1), 100.92(2); O(1)−N(1)−Fe, 172.8(2); O(2)−N(2)−Fe, 167.4(3).

Conclusion and Comments. Studies on the neutral {Fe(NO)$_2$}^{10} **1**, **2**, the anionic {Fe(NO)$_2$}^{9} **4**, and the cationic {Fe(NO)$_2$}^{9} **3** have resulted in the following conclusions.

(1) The facile transformation of the neutral complex **1** to the anionic complex **4** may occur via the cationic complex **3**. That is, the cationic {Fe(NO)$_2$}^{9} complex **3** acts as an [Fe(NO)$_2$]-donor reagent in the presence of thiolates or $[(RS)_2Fe(NO)_2]^-$.

(2) This result in combination with the previous study shows that the stability of the anionic $[(RS)_2Fe(NO)_2]^-$ was finely modulated by the electronic and structural environments of the coordinated thiolate ligands.[10c] The bidentate alkylthiolate-coordinated ligand of complex **4** promotes the stability of the anionic {Fe(NO)$_2$}^{9} DNICs compared to the monodentate alkylthiolate-coordinated ligands. The chelating

Table 2. Selected IR Data for the Neutral $\{Fe(NO)_2\}^{10}$ and the Anionic/Neutral/Cationic $\{Fe(NO)_2\}^9$ DNICs

complex	ν_{NO} (cm^{-1})	$\Delta\nu_{NO}$ (cm^{-1})	ref
Neutral $\{Fe(NO)_2\}^{10}$ DNICs			
1	1622, 1679[e]	57	this work
2	1644, 1698[a]	54	this work
$[(1\text{-MeIm})_2Fe(NO)_2]$	1616, 1673[b]	57	9
$[(PPh_3)_2Fe(NO)_2]$	1678, 1724[c]	46	8a
Anionic $\{Fe(NO)_2\}^9$ DNICs			
4	1671, 1712[a]	41	this work
$[S_5Fe(NO)_2]^-$	1695, 1739[a]	44	10b
$[(2\text{-}S{-}(C_4H_3S)_2Fe(NO)_2]^-$	1698, 1743[a]	45	10c
$[(2\text{-}S{-}C_7H_4NS)_2Fe(NO)_2]^-$	1716, 1766[a]	50	10c
$[(SC_6H_4\text{-}o\text{-}NHCOCH_3)_2Fe(NO)_2]^-$	1705, 1752[a]	47	10c
$[(SePh)_2Fe(NO)_2]^-$	1697, 1741[d]	44	18
$[Se_5Fe(NO)_2]^-$	1697, 1736[a]	39	10d
Cationic $\{Fe(NO)_2\}^9$ DNICs			
3	1746, 1814[e]	68	this work
$[(6\text{-}Me_3\text{-TPA})Fe(NO)_2]^+$	1726, 1801[e]	75	17
$[(OPPh_3)_2Fe(NO)_2]^+$	1734, 1813[d]	79	14
$[(PPh_3)(OPPh_3)Fe(NO)_2]^+$	1746, 1809[d]	63	14
Neutral $\{Fe(NO)_2\}^9$ DNIC			
$[(SC_6H_4\text{-}o\text{-}NHCOPh)(Im)Fe(NO)_2]$	1722, 1786[a]	64	10a
$[(H^+bme\text{-}daco)Fe(NO)_2]$	1740, 1696[a]	44	6a
$[(C_9H_{21}N_2S_2)Fe(NO)_2]$	1740, 1695[d]	45	6b

[a] THF. [b] Diethyl ether. [c] Tetrachloroethylene. [d] CH_2Cl_2. [e] CH_3CN.

effect overwhelming the S-donating ability (electronic effect) may rationalize the observed isolation/stability of complex **4**.

(3) On the basis of N−O and Fe−N(O) bond lengths of the single-crystal X-ray structures of the $\{Fe(NO)_2\}^9$/$\{Fe(NO)_2\}^{10}$ DNICs, the mean N−O distances fall in the range of 1.214(6)−1.189(4) Å and the mean Fe−N(O) distances are within the range of 1.650(7)−1.638(3) Å for the neutral $\{Fe(NO)_2\}^{10}$ DNICs (Table 1).[8,9] In contrast, the mean N−O distances ranging from 1.178(3) to 1.160(6) Å and the mean Fe−N(O) distances ranging from 1.695(3) to 1.661(4) Å are assigned as the anionic/neutral/cationic $\{Fe(NO)_2\}^9$ DNICs (Table 1).[6−10,17,1817−18] Obviously, complex $[(6\text{-}Me_3\text{-TPA})Fe(NO)_2]^+$ is best described as a cationic $\{Fe(NO)_2\}^9$ DNIC (Table 1).[17]

(4) EPR spectra in combination with IR ν_{NO} spectra (the relative position of the ν_{NO} stretching frequencies and their difference $\Delta\nu_{NO} \sim 45$ cm^{-1} for the EPR-active, anionic $\{Fe(NO)_2\}^9$ DNICs, ~65 cm^{-1} for the EPR-active, cationic $\{Fe(NO)_2\}^9$ DNICs, ~55 cm^{-1} for the EPR-silent, neutral $\{Fe(NO)_2\}^{10}$ DNICs, and ~64 cm^{-1} for the EPR-active, neutral $\{Fe(NO)_2\}^9$ DNICs) may serve as an efficient tool for discrimination of the existence of the anionic $\{Fe(NO)_2\}^9$, the cationic $\{Fe(NO)_2\}^9$, the neutral $\{Fe(NO)_2\}^9$, and the neutral $\{Fe(NO)_2\}^{10}$ DNICs (Table 2).[6−18]

In this study, the isolation of complex **4**, mimicking Cys−$(X)_n$−Cys binding of $Fe(NO)_2$ to proteins or thiobiomolecules, implicates that the chelating effect of thiobiomolecules or proteins may play a key role in creating/stabilizing the protein-bound DNICs.[5,6] The reversible conversion from complex **4** to complex **6** may decipher the protein-bound DNICs mobilized by the reaction with thiol such as glutathione or free cysteine to form LMW-DNICs.[5,6]

Experimental Section

Manipulations, reactions, and transfers were conducted under N_2 according to Schlenk techniques or in a glovebox (Ar gas). Solvents were distilled under N_2 from appropriate drying agents (diethyl ether from CaH_2; acetonitrile from CaH_2/P_2O_5; methylene chloride from CaH_2; hexane and THF from sodium benzophenone) and stored in dried, N_2-filled flasks over 4-Å molecular sieves. N_2 was purged through these solvents before use. The solvent was transferred to the reaction vessel via a stainless cannula under positive pressure of N_2. The reagents sparteine, TMEDA, thiophenol, iron pentacarbonyl, 1,3-propanedithiol (Aldrich), and bis(triphenylphosphoranylidene)ammonium chloride ([PPN][Cl]; Fluka) were used as received. Compound $[PPN][Fe(CO)_3(NO)]$ was synthesized by published procedures.[13] IR spectra of the ν_{NO} stretching frequencies were recorded on a PerkinElmer model spectrum one B spectrometer with sealed solution cells (0.1 mm, KBr windows). ^1H NMR spectra were obtained on a Varian Unity-500 spectrometer. UV−vis spectra were recorded on a Jasco V-570 spectrometer. Analyses of C, H, and N were obtained with a CHN analyzer (Heraeus).

Preparation of [(Spartiene)Fe(NO)$_2$] (Sparteine = $C_{15}H_{26}N_2$; 1). Sparteine (40 μL, $d = 1.02$ g mL^{-1}, 0.2 mmol) was added into the THF solution of $[Fe(CO)_2(NO)_2]$,[13] freshly prepared from the reaction of $[PPN][Fe(CO)_3(NO)]$ (0.141 g, 0.2 mmol) and $[NO][BF_4]$ (0.024 g, 0.2 mmol), and stirred for 4 h under N_2 at ambient temperature. The reaction was monitored with FTIR. The IR spectrum [ν_{NO} 1633 and 1687 cm^{-1} (THF)] was assigned to the formation of **1**. Diffusion of hexane into the THF solution of complex **1** at −15 °C led to green crystals **1** (0.082 g, 35%) suitable for single-crystal X-ray diffraction. IR: ν_{NO} 1633, 1687 cm^{-1} (THF); 1622, 1679 cm^{-1} (CH_3CN). ^1H NMR (CD_3CN): δ 4.06 (d, $C(15)H_A$, not first order), 3.68 (m, $C(2)H_A$), 3.34 (m, $C(17)H_A$), 3.02 (m, $C(10)H_A$), 2.86 (m, $C(17)H_B$), 2.62 (m, $C(15)H_B$), 2.52 (m, $C(10)H_B$), 2.21 (m, $C(2)H_B$), 2.00 (m, $C(8)H_A$, C(11)H), 1.87 (m, C(9)H), 1.81−1.61 (m) (C(6)H, $C(4)H_A$, and $C(13)H_A$), 1.60−1.25 (m, $C(3)H_2$, $C(14)H_2$, $C(12)H_A$, C(7)H), 1.24−1.17 (m, $C(5)H_2$, $C(12)H_B$, $C(4)H_B$, and $C(13)H_B$), 0.96 (m, $C(8)H_B$). Absorption spectrum (THF) [λ_{max}, nm (ϵ, M^{-1} cm^{-1})]: 366 (816), 392 (781), 518 (143), 722 (113). Anal. Calcd for $C_{15}H_{26}N_4O_2Fe$: C, 51.39; H, 7.42; N, 15.99. Found: C, 50.65; H, 8.05; N, 15.32.

Preparation of [(TMEDA)Fe(NO)$_2$] (TMEDA = *N,N,N′,N′*-Tetramethylethenediamine; 2). TMEDA (30 μL, $d = 0.775$ g mL^{-1}, 0.2 mmol) was added into the THF solution of $[Fe(CO)_2(NO)_2]$, and the reaction solution was stirred for 4 h under N_2 at ambient temperature. The reaction was monitored with FTIR. IR spectrum [ν_{NO} 1644 and 1698 cm^{-1} (THF)] was assigned to the formation of **2**. Diffusion of hexane into the THF solution of complex **2** at −15 °C led to green crystals **2** suitable for single-crystal X-ray diffraction (yield 0.056 g, 24%). IR: ν_{NO} 1644, 1698 cm^{-1} (THF). ^1H NMR (C_4D_8O): δ 2.75 (s, CH_2), 2.52 (s, CH_3). Absorption spectrum (THF) [λ_{max}, nm (ϵ, M^{-1} cm^{-1})]: 369 (501), 388 (489), 508 (87), 726 (47). Anal. Calcd for $C_6H_{16}N_4O_2Fe$: C, 31.02; H, 6.94; N, 24.14. Found: C, 30.43; H, 6.29; N, 24.03.

Preparation of [(Sparteine)Fe(NO)$_2$][BF$_4$] (3). 1 (0.035 g, 0.1 mmol) and $[NO][BF_4]$ (0.012 g, 0.1 mmol) were dissolved in CH_3CN and stirred for 5 min under N_2 at ambient temperature. The reaction was monitored with FTIR. IR [ν_{NO} 1746 and 1814 cm^{-1} (CH_3CN); 1739 and 1808 cm^{-1} (THF)] and EPR (an isotropic $g =$ 2.032 signal at 298 K, characteristic of LMW-DNICs) spectra

(17) Jo, D.-H.; Chiou, Y.-M.; Que, L., Jr. *Inorg. Chem.* **2001**, *40*, 3181−3190.
(18) Liaw, W.-F.; Chiang, C.-Y.; Lee, G.-H.; Peng, S.-M.; Lai, C.-H.; Darensbourg, M. Y. *Inorg. Chem.* **2000**, *39*, 480−484.

identified the formation of **3**.[14] Absorption spectrum (CH_3CN) [λ_{max}, nm (ϵ, M^{-1} cm^{-1})]: 371 (1061), 525 (264), 1105 (58).

Preparation of [PPN][(S(CH$_2$)$_3$S)Fe(NO)$_2$] (4). Method A. A THF solution of $Fe(CO)_2(NO)_2$, freshly prepared from the reaction of [PPN][$Fe(CO)_3(NO)$] (0.071 g, 0.1 mmol) and [NO][BF_4] (0.012 g, 0.1 mmol),[13] was transferred to a 50-mL Schlenk flask loaded with $HS(CH_2)_3SH$ (10 μL, 0.1 mmol) by a cannula under positive N_2 pressure at room temperature. The reaction solution was stirred at room temperature overnight. The IR spectrum (ν_{NO} 1749 s, 1775 s, and 1806 vw cm^{-1}) shows the formation of [$Fe_2(\mu$-$S(CH_2)_3S)(NO)_4$].[10a,15] The THF solution (10 mL) of [$Fe_2(\mu$-$S(CH_2)_3S)(NO)_4$] (0.05 mmol) was transferred to [PPN]$_2$[$S(CH_2)_3S$] (0.118 g, 0.1 mmol) by a cannula and stirred for 20 min. The resulting mixture was filtered through Celite to separate the insoluble solid. The resulting solution was then concentrated, and diethyl ether and hexane (5 and 15 mL, respectively) were added to precipitate the dark-brown solid [PPN]**4** (yield 0.06 g, 78%). Diffusion of diethyl ether into the THF solution of complex **4** at 0 °C for 1 week led to dark-brown crystals suitable for single-crystal X-ray diffraction. **Method B.** The acetonitrile solution of complex **3**, freshly prepared from the reaction of complex **1** (0.035 g, 0.1 mmol) and [NO][BF_4] (0.012 g, 0.1 mmol), was transferred to a 50-mL Schlenk flask loaded with [PPN]$_2$[$S(CH_2)_3S$] (0.236 g, 0.2 mmol) by a cannula under positive N_2 pressure at ambient temperature. The reaction mixture was stirred for 10 min. The resulting mixture was dried under vacuum and then redissolved in THF. The resulting mixture was filtered through Celite to separate the insoluble solid. The solution was then concentrated, and diethyl ether and hexane (5 and 15 mL, respectively) were added to precipitate dark-brown solid [PPN]**4** (yield 0.0479 g, 63%). IR: ν_{NO} 1671, 1712 cm^{-1} (THF); 1676, 1718 cm^{-1} (CH_3CN). Absorption spectrum (THF) [λ_{max}, nm (ϵ, M^{-1} cm^{-1})]: 366 (5680), 430 (3837), 578 (1211), 807 (371). Anal. Calcd for $C_{39}H_{36}N_3O_2S_2P_2Fe$: C, 61.53; H, 4.73; N, 5.52. Found: C, 60.97; H, 5.25; N, 4.93.

Addition of 3 to [PPN]6. An acetonitrile solution of complex **3**, freshly prepared from the reaction of complex **1** (0.035 g, 0.1 mmol) and [NO][BF_4] (0.012 g, 0.1 mmol) in CH_3CN, was added into [PPN]**6** (0.218 g, 0.1 mmol) via a cannula under positive N_2 pressure. The reaction solution was stirred for 5 min under N_2 at ambient temperature. The reaction was monitored with FTIR. The IR spectrum [ν_{NO} 1759 s, 1786 s, and 1817 w cm^{-1} (CH_3CN); 1749 s, 1775 s, and 1806 w cm^{-1} (THF)] was assigned to the formation of [$Fe_2(\mu$-$SPh)_2(NO)_4$] (**5**).[15] The solution was dried under vacuum, and diethyl ether was added to redissolve the solid. The reacting mixture was then filtered through Celite to separate the insoluble solid. The final solution was dried under the vacuum to yield **5** (yield 0.044 g, 97%).

Reaction of 5 and [PPN][SPh]. A THF solution (10 mL) of complex **5** (0.045 g, 0.1 mmol) was transferred to a 50-mL Schlenk flask loaded with [PPN][SPh] (0.129 g, 0.2 mmol) by a cannula under positive N_2 pressure at room temperature. The reaction mixture was stirred for 5 min at room temperature and then filtered through Celite to separate the insoluble solid. The solution was concentrated, and diethyl ether and hexane (5 and 15 mL, respectively) were added to precipitate the dark-red solid [PPN]**6** (yield 0.075 g, 86%) characterized by IR [ν_{NO} 1693 and 1737 cm^{-1} (THF)] UV−vis [absorption spectrum (THF) [λ_{max}, nm (ϵ, M^{-1} cm^{-1})]: 363 (4065), 484 (1991), 800 (473)].[10c,16]

Addition of 3 to [PPN][SPh]. An acetonitrile solution of complex **3**, freshly prepared from the reaction of complex **1** (0.035 g, 0.1 mmol) and [NO][BF_4] (0.012 g, 0.1 mmol) in CH_3CN, was added into [PPN][SPh] (0.130 g, 0.2 mmol) via a cannula under positive N_2 pressure. The reaction solution was stirred for 5 min under N_2 at ambient temperature. The reaction mixture was dried under vacuum, and then diethyl ether was added to abstract the red-brown product. Hexane was added to precipitate the product [PPN]**6** (yield 68%) characterized by IR and UV−vis.[10c,16]

Reaction of [PPN]6 and [PPN]$_2$[S(CH$_2$)$_3$S]. A THF solution (10 mL) of complex **6** (0.087 g, 0.1 mmol) was transferred to a 50-mL Schlenk flask loaded with [PPN]$_2$[$S(CH_2)_3S$] (0.118 g, 0.1 mmol) by a cannula under positive N_2 pressure at room temperature. The reaction solution was stirred for 30 min at room temperature, and the resulting mixture was filtered through Celite to separate the insoluble solid. The solution was then concentrated, and diethyl ether and hexane (5 and 15 mL, respectively) were added to precipitate the dark-brown solid [PPN]**4** (yield 0.0669 g, 88%) characterized by IR and UV−vis.

Reaction of [PPN]4 and Thiophenol. Complex **4** (0.076 g, 0.1 mmol) and thiophenol (20 μL, 0.2 mmol) were dissolved in THF (15 mL) under a N_2 atmosphere. The reaction mixture was stirred at room temperature for 1 h, and the resulting solution was filtered through Celite. The solution was then concentrated under vacuum, and diethyl ether and hexane (5 and 15 mL, respectively) were added to precipitate dark-red solid [PPN]**6** (yield 0.0716 g, 82%) characterized by IR and UV−vis.

EPR Measurements. EPR measurements were performed at the X band using a Bruker EMX spectrometer equipped with a Bruker TE102 cavity. The microwave frequency was measured with a Hewlett-Packard 5246L electronic counter. X-band EPR spectra of complexes **3** and **4** in THF were obtained with a microwave power of 20.020 mW, a frequency of 9.605 GHz, and a modulation amplitude of 0.2 G at 100 kHz.

Magnetic Measurements. The magnetic data were recorded on a SQUID magnetometer (MPMS5 Quantum Design Company) under a 1-T external magnetic field in the temperature range of 4−300 K. The magnetic susceptibility data were corrected with temperature-independent paramagnetism (2×10^{-4} cm^3 mol^{-1}) and ligands' diamagnetism by the tabulated Pascal's constants.

Crystallography. Crystallographic data and structural refinement parameters of complexes **1**, **2**, and **4** are summarized in the Supporting Information (Tables S1−S3). Each crystal was mounted on a glass fiber and quickly coated with an epoxy resin. Unit-cell parameters were obtained by least-squares refinement. Diffraction measurements for complexes **1**, **2**, and **4** were carried out on a SMART Apex CCD diffractometer with graphite-monochromated Mo Kα radiation (λ = 0.7107 Å). Least-squares refinement of the positional and anisotropic thermal parameters of all non-H atoms and fixed H atoms was based on F^2. A *SADABS*[19] absorption correction was made. The *SHELXTL*[20] structural refinement program was employed.

Acknowledgment. We gratefully acknowledge financial support from the National Science Council (Taiwan).

Supporting Information Available: Crystallographic data and structural refinement parameters for complexes **1**, **2**, and **4** and X-ray crystallographic files in CIF format for the structural determinations of **1**, [$(CH_3)_2N(CH_2)_2N(CH_3)_2$)Fe$(NO)_2$], and [PPN]-**4**. This material is available free of charge via the Internet at http://pubs.acs.org.

IC0605120

(19) Sheldrick, G. M. *SADABS, Siemens Area Detector Absorption Correction Program*; University of Göttingen: Göttingen, Germany, 1996.
(20) Sheldrick, G. M. *SHELXTL, Program for Crystal Structure Determination*; Siemens Analytical X-ray Instruments Inc.: Madison, WI, 1994.